REVISTA INTERDISCIPLINAR DE PESQUISA EM ENGENHARIA

CILAMCE 2016
XXXVII IBERIAN LATIN AMERICAN CONGRESS ON COMPUTATIONAL METHODS IN ENGINEERING
BRASÍLIA - DF - BRAZIL

NUMERICAL INVESTIGATIONS OF INSTABILITIES IN GAS-SOLID FLUIDIZED BEDS

Shyam Sumanta Das

Yuri Dumaresq Sobral

das.shyamsumanta@gmail.com

ydsobral@unb.br

Departamento de Matematica, Instituto de Ciencias Exatas, Universidade de Braslia, Campus Universitario Darcy Ribeiro, 70910-900, DF, Brazil

Francisco Ricardo da Cunha

frcunha2@gmail.com

Departamento de Engenharia Mecanica, Faculdade de Tecnologia, Universidade de Braslia, Campus Universitario Darcy Ribeiro, 70910-900, DF, Brazil

Abstract. A gas-solid fluidized bed consists of mixture of gas-solid in which the particles were suspended by an imposed upward flow. In the present paper, we have carried out two dimensional numerical simulations of gas-solid fluidized bed. CFD-DEM (Computational fluid dynamics-discrete element modeling) approach is used to model two phase flow composed of solid particles and gas inside the fluidized bed. It uses Eulerian and Lagrangian methods to solve fluid and solid particles respectively. Numerical simulations were carried out for various inlet gas velocities. The aim of the present work to investigate the instabilities associated with the fluidized bed. Spectral analyses were carried out to investigate the nature of the signals. The appearance of the bubble kind structure in the fluidized bed within few seconds of injection of gas shows the occurrence of instability in the fluidized bed system. This instability give rise to the formation bubbles of different sizes.

Keywords: *Fluidized bed, Computational fluid dynamics, discrete element modeling*

1 INTRODUCTION

Gas-solid fluidized beds are widely used in chemical, petrochemical, metallurgical, environmental and energy industries in large scale operations such as coating, granulation, drying. One of the major advantage of fluidized beds lie in good gas-solid mixing, results in uniform temperature distribution and high rate of heat transfer between bed and an immersed heating surface in the bed. A gas-solid fluidized bed consists of mixture of gas-solid in which the particles were suspended by an imposed upward flow. Fluidization occurs when a gas is pushed upwards through a bed of particles. At a low superficial gas velocity, the drag on each particle is also low, and thus bed height remains unchanged. As the superficial gas velocity increases in the reactor, the pressure drop across the bed also increases. Then, at a certain gas velocity, the upward drag force equals to weight of the bed and the particles are free to move. Then, the bed is said to be fluidized. Lack of understating of the fundamental of dense gas-particulate flows in general has lead to severe difficulties in design and scaling up the reactor in industrial scale. Also, in most of cases, the design and scale up of fluidized bed reactors is fully an empirical process based on the primitive studies in pilot scale models which is a time consuming process.

In this scenario, computational fluid dynamics (CFD) will be a very useful tool in understanding the complex physical process associated with the fluidized bed reactors. With the increase in the computer technology over the years, it is now possible to simulate the complex dense particulate flows. Generally, there are two different kinds of approaches to model the gas-solid flows (1) Eulerian-Eulerian (EE) (2) Eulerian-Lagrangian (EL) approach. In Eulerian-Eulerian approach, the gas and the solid are treated as interpenetrating continua. Continuity and momentum equations are written for each phase, and interphase interaction is accounted for through appropriate sources and sinks in the phase momentum equations. This approach requires a constitutive equation for the solid phase to relate the solids stress tensor to the velocity field; the fluid phase is typically modeled as Newtonian. The interphase interaction terms typically involve empirical relationships for drag, heat transfer and other exchanges. In Eulerian-Lagrangian approach, the fluid flow is solved using the continuum equations, and the particulate phase flow is described by tracking the motion of individual particles (Tsuji et al., 1993). Discrete particle models (DPM) have been used for a wide range of applications (Tsuji et al., 1993).

The study of stability in a fluidized bed aims to indentify the hydrodynamic mechanisms that cause the appearance of the bubbles in these flows. Bubbles are large regions void of particles that travel upstream and alter significantly the pattern of the flow. Therefore, it is extremely important to identify the mechanism behinds bubble formation in order to be able to better understand and control such flows. Over the years several researchers carried out stability analysis for the study of stability in a fluidized bed (El-Kassy and Homsy., 1975; Sobral and Cunha.,2002; Anderson et al., 1995; Sobral., 2008). In a classical work, Anderson and Jackson (1967) used the local averaged equations for momentum and continuity equations. The averaged equations are perturbed with small disturbances from the homogeneous fluidization state, and linearized with respect to the perturbations. The author carried out a stability analysis and observed that the particle pressure term has a stabilizing effect and that the particle viscosity acts as a short wave filter.

Some authors (El-Kassy and Homsy., 1975) performed experimental studies in a liquid-solid fluidized bed to investigate the origin of bubbles. They observed that, although the waves experiences an initially exponential growth in amplitude, the ultimate state of motion exhibited is that complicated formation and destruction of cylindrical bubbly like structures. Expected values of their amplitude, frequency, and velocity were measured and preliminary scaling laws were proposed. Glassier et al. (1996) carried out numerical continuation

technique as well as bifurcation theory, both one and two dimensional wave solutions of the ensemble –averaged equation of motion for gas and particles in fluidized beds. They have observed that, the presence of vertical structure emerge through Hopf bifurcation of the uniform state and two dimensional wave solutions were born out of one dimensional waves. The fully developed two dimensional waves are reminiscent of bubbles. They found that the qualitative features of the bifurcation diagram are not affected by changes in the model parameters or the closures. An examination of the stability of one dimensional wave solutions to two dimensional perturbations suggests that two-dimensional solutions emerge through a mechanism which is similar to the overturning instability analyzed by Batchelor and Nitsche (1991).

Sobral and Hinch (2011) studied the stability of stratified particulate flows to transverse disturbances, leading to gravitational overturning. They have used a one-fluid model in which particles are responsible for the stratification of the flow but do not slip relative to the fluid and do not diffuse. A linear stability analysis and a numerical simulation of the governing equations were performed in order to determine and characterize the instability of the flow. They observed that stratified flows are unstable to transverse disturbances and that the instability is driven by a tilt-and-slide mechanism that creates ascending regions of low concentration of particles and descending regions of high concentration of particles. This mechanism might be related to the formation of bubbles in fluidized beds.

Linear stability analysis was carried out by Cunha et al. (2013) to evaluate the behavior of concentration waves in polarized fluidized beds. They proposed a non linear model for the fluid-particle interaction force, so that the inertial effects arising from wakes behind the particles are incorporated. They observed that, the growth rate instabilities are considerably reduced when a magnetic field is applied in a fluidized bed of magnetic particles, this effect being most efficient. When the applied field is perpendicular to the flow, there is only a small reduction of growth rates. They also observed that, wake interaction mechanism and the particle pressure are stabilizing mechanisms and that the magnetic field intensities necessary for full stabilization when these terms were not included in the model are greater than those compared to predictions made with these terms in the model.

CFD-DEM (Computational fluid dynamics-discrete element modeling) simulation was carried out by Das et al. (2016) to model two phase flow composed of solid particles and gas inside the fluidized bed. Gigaspow drag model was used to model the interaction between gas and solid particles. Numerical simulations were performed for various inlet gas velocities (0.75 m/s to 0.82 m/s) for the fluidized bed. They have investigated the stability of the fluidized bed by analyzing amplitude of the disturbances. They observed that, the amplitude of disturbances increases with the increase in bed height. Further, they found that growth rate of the amplitude of disturbances is linear for v_g = 0.75 to 0.80 m/s and nonlinear for v_g = 0.82 m/s.

In the present work, the flow behavior of solid phases is simulated by means of CFD-DEM in a gas–solid fluidized bed with using MFIX code. The aim of the present work is to see the study instability associated with the fluidized bed. Numerical simulations were carried out at different inlet gas velocities. Further, a spectral analysis study was carried out to investigate the nature of the signals.

2 MATHEMATICAL MODEL

In the present study, fluid motion is solved using volume averaged equations (Anderson and Jackson., 1967) and particle motion is modeled by using spring-dashpot model (Cundall and Strack., 1979).

2.1 Governing equations

Particle motion

The equation for both translational and rotational motion for the i^{th} particle are given by

$$\frac{d\vec{x_i}}{dt} = \vec{v_i} \tag{1}$$

$$m_i \frac{d\vec{v_i}}{dt} = m_i \vec{g} + \sum_{\substack{i,j=1 \\ i \neq j}}^{N} \vec{F}_{i,j}^{(C)} + \vec{F}_i^{(d)} \tag{2}$$

$$I_i \frac{d\vec{\omega_i}}{dt} = \sum_{\substack{i,j=1 \\ i \neq j}}^{N} \vec{\tau}_{ij} \tag{3}$$

The mass, position vector and velocity vector for the i^{th} particle is given by m_i, , $\vec{x_i}$, $\vec{v_i}$ and $\vec{g}$ the acceleration due to gravity.

$$\vec{F}_{i,j}^{(C)} = \sum_{\substack{i,j=1 \\ i \neq j}}^{N} \left(\vec{F}_{i,j}^{(n)} + \vec{F}_{i,j}^{(\tau)} \right) \tag{4}$$

The contact forces, normal and tangential component between i^{th} and j^{th} partcile are given by $\vec{F}_{i,j}^{(C)}$, $\vec{F}_{i,j}^{(n)}$, $\vec{F}_{i,j}^{(\tau)}$. The total drag force is given by $\vec{F}_i^{(d)}$. I_i, $\vec{\omega_i}$, and $\vec{\tau}_{ij}$ are the moment of inertia, angular velocity and torque acting on the i^{th} particle.

$$\vec{F}_{i,j}^{(n)} = -k.\vec{\delta}_{ij}^{(n)} - \eta \left(\vec{v}_{rij}.\vec{n}_{ij} \right).\vec{n}_{ij} \tag{5}$$

$$\vec{v}_{rij} = \vec{v}_i - \vec{v}_j \tag{6}$$

$$\vec{F}_{i,j}^{(\tau)} = -k.\vec{\delta}_{ij}^{(\tau)} - \eta \left(\vec{v}_{rij}.\vec{n}_{ij} \right).\vec{n}_{ij} \tag{7}$$

$$\vec{F}_i^{(d)} = -\vec{\nabla} p + \vec{f}_{gp} \tag{8}$$

$\vec{\delta}_{ij}^{(n)}, \vec{\delta}_{ij}^{(\tau)}$ are the normal and tangential overlapping distance between particle i^{th} and j^{th} particles, respectively. k and η are the stiffness constant for the spring and viscous damping coefficient. $\vec{v}_{rij}$ is the relative velocity between i^{th} and j^{th} particle and $\vec{n}_{ij}$ is the unit normal vector along $\vec{v}_{rij}$.

Gas phase

$$\frac{\partial\left(\varepsilon_g \rho_g\right)}{\partial t}+\frac{\partial}{\partial x_j}\left(\varepsilon_g \rho_g u_j\right)=0 \tag{9}$$

$$\frac{\partial}{\partial t}\left(\varepsilon_g \rho_g u_i\right)+\frac{\partial}{\partial x_j}\left(\varepsilon_g \rho_g u_j u_i\right)=-\frac{\partial p}{\partial x_i}+\frac{\partial}{\partial x_j}\left[\mu_g\left(\frac{\partial u_i}{\partial x_j}\right)\right]+f_{gp}+\varepsilon_g \rho_g g \tag{10}$$

The local mean void fraction is given by ε_g. u_i is the local mean gas velocities, ρ_g is the gas density, p is the local mean gas pressure, f_{gp} is the force of interaction between gas and solid particles (drag force).Various models of gas-particle interactions were proposed by researchers. The volumetric gas particle interaction is given by

$$f_{gp}=\beta\left(v_p-u_i\right) \tag{11}$$

Where, v_p is the particle velocity and u_i is the volume averaged gas velocity, β is the fluid particle interaction coefficient. In the present work, Gidaspow drag model is used for the modeling the interaction between gas and the particles phase.

$$\beta=\begin{cases}\dfrac{1-\varepsilon_g}{d_p^2 \varepsilon_g}\left\{150\dfrac{\left(1-\varepsilon_g\right)}{d_p}+1.75\rho_g \varepsilon_g\left|\vec{v_s}-\vec{u}\right|\right\}, \left(\varepsilon_g \le 0.8\right) \\ \dfrac{3}{4}C_D\dfrac{\left|\vec{v_s}-\vec{u}\right|\rho_g\left(1-\varepsilon_g\right)}{d_p}\varepsilon_g{}^{-27}, \left(\varepsilon_g > 0.8\right)\end{cases} \tag{12}$$

$$C_D=\begin{cases}24\dfrac{\left(1+0.15\,\mathrm{Re}^{0.687}\right)}{\mathrm{Re}} & ,\mathrm{Re}<1000 \\ 0.48 & ,\mathrm{Re}>1000\end{cases} \tag{13}$$

$$\mathrm{Re}=\frac{\left|\vec{v_s}-\vec{u}\right|\rho_g \varepsilon_g d_p}{\mu} \tag{14}$$

The diameter of the particle is given by d_p. Where, μ is the dynamic viscosity, $\vec{v_s}$ is the particle velocity in the averaged cell. The fluid motion was solved simultaneously with the motion of the particles. Initially, the equations for gas motion are solved. Then, the drag force for each particle is calculated using local gas velocity and particle velocity. Two dimensional CFD-DEM simulations were performed for a fluidized bed using open source MFIX-DEM code(SyamLal.,1998). Hexahedral cell elements were used for meshing the geometry. Finite volume method (FVM) was used in code to discretize the governing equations (Patankar, 1980). MUSCL (Monotonic Upstream-Centered Scheme for Conservation Laws) scheme (VanLeer., 1979) was used to model the convective terms in the momentum equations. The convergence criterion was set at 10^{-4} for all the dependent variables. SIMPLE algorithm (Patankar.,1980) was used for pressure-velocity coupling. BICGTAB (Biconjugate gradient method) was considered for solving the linear equations. First order Euler integration method was used for time discretization. It was earlier reported from the work of Tsuji et al. (1993)

that, the time step size in DES simulation depends on the stiffness. Therefore, in the present simulation, Δt = 0.0002 s is considered. For each time step, convergence criteria were set at 10^{-4} for all the dependent variables. Numerical simulations were performed for 25 s. The inlet boundary of the domain was defined as the velocity inlet. Whereas, at the outlet, pressure outlet boundary condition was used. No slip boundary condition was used at the wall. Further, an in-house MATLAB code was developed to calculate Fast Fourier Transform (FFT) of the signals.

3. RESULTS AND DISCUSSION

In the present section, the results obtained from numerical simulations from a two dimensional fluidized bed has been presented. Table1. shows the simulation parameters for the fluidized bed simulations. Initially, the magnetic effects on the fluidized bed are not considered. As shown in table 1. Simulations were performed in the velocity range u_g= 0.26 m/s to 0.28 m/s. In the present work, simulation results for u_g= 0.26 m/s and 0.28 m/s were presented. All the parameters in the table were presented in SI units.

Table 1: Simulation parameters for fluidized bed simulations

Constitutive relation	Nomenclature	Value
Bed dimension	*(WxH)*	0.08 x 0.88
Fluid mesh size		8x88
Cell dimensions		0.01 x 0.01
Gas velocity at the inlet	u_g	0.26 to 0.28
Gas density:	ρ_g	1.205
Gas viscosity:	μ_g	1.800E-5
Number of particles:	N_p	1900
Particle density:	ρ_g	2700
Particle diameter:	d_p	0.004
Particle stiffness coefficient	k	1e+06
Particle coefficient of restitution	e	0.9
Friction damping coeffcient	η	0.1

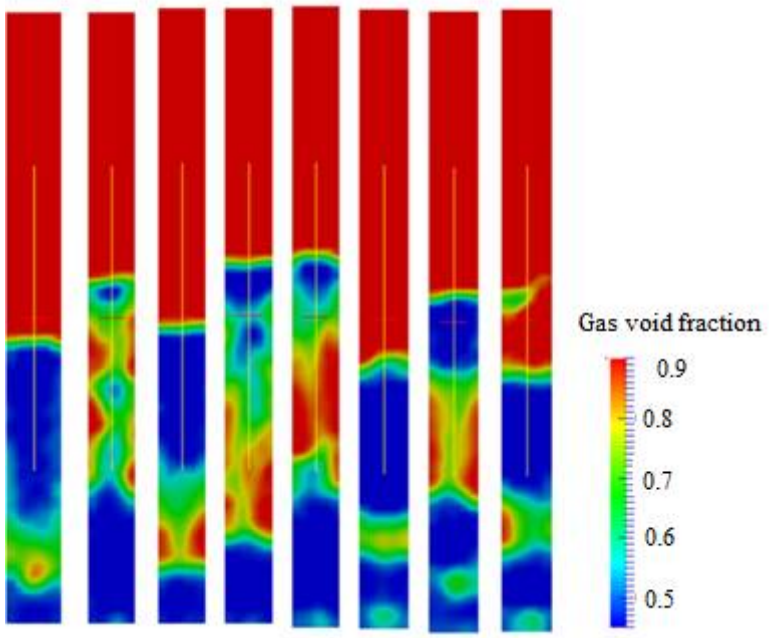

(a) (b) (c) (d) (e) (f) (g) (h)

Figure. 1: Gas volume fraction contours for u_g = 0.26 m/s (a) 0.48 s (b) 0.76 s (c) 1.79s (d) 2.76s (e) 6.24s (f) 8.44s (g) 12.33s (h) 14.17s

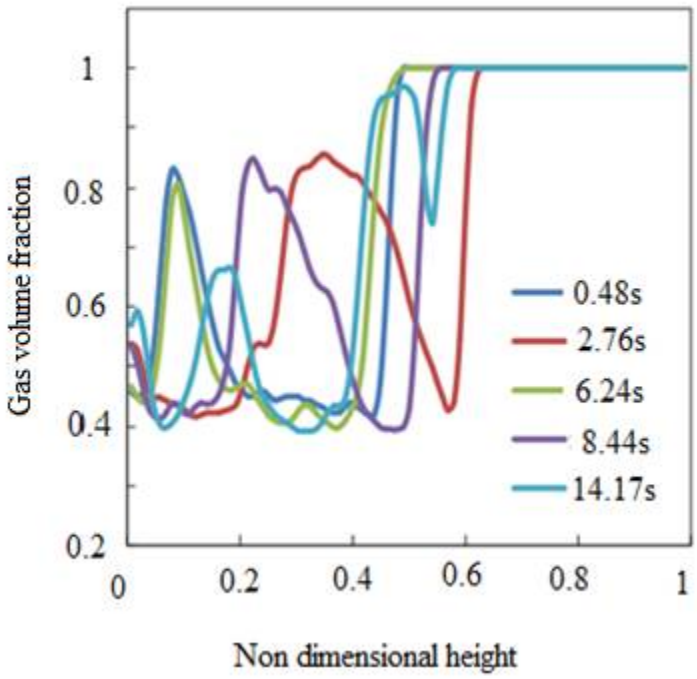

Figure. 2: Variation of gas volume fraction (ε_g) profile with non dimensional height at different times for u_g = 0.26 m/s

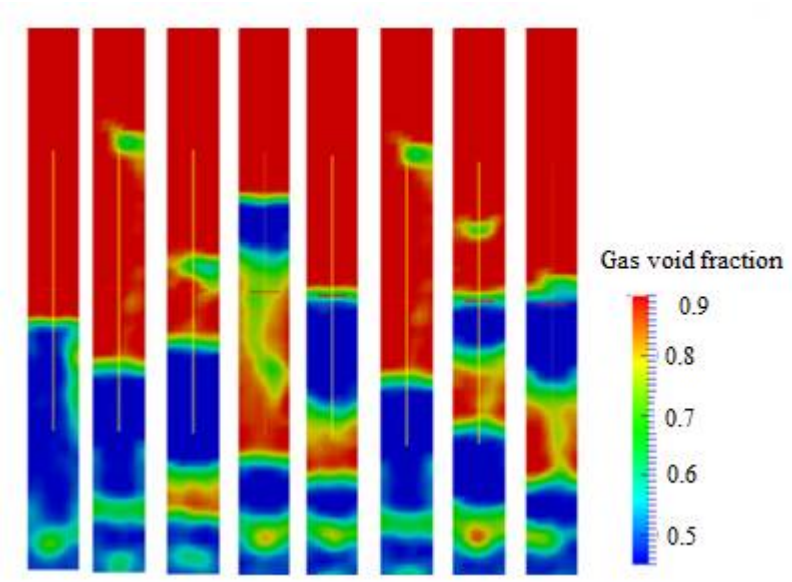

(a) (b) (c) (d) (e) (f) (g) (h)

Figure. 3: Gas volume fraction contours (a) 0.3 s (b) 0.93 s (c) 2.01 s (d) 2.43s (e) 6.68s (f) 8.44s (g) 11.41 s (g) 14.01s (h) 16.5s for u_g = 0.28 m/s

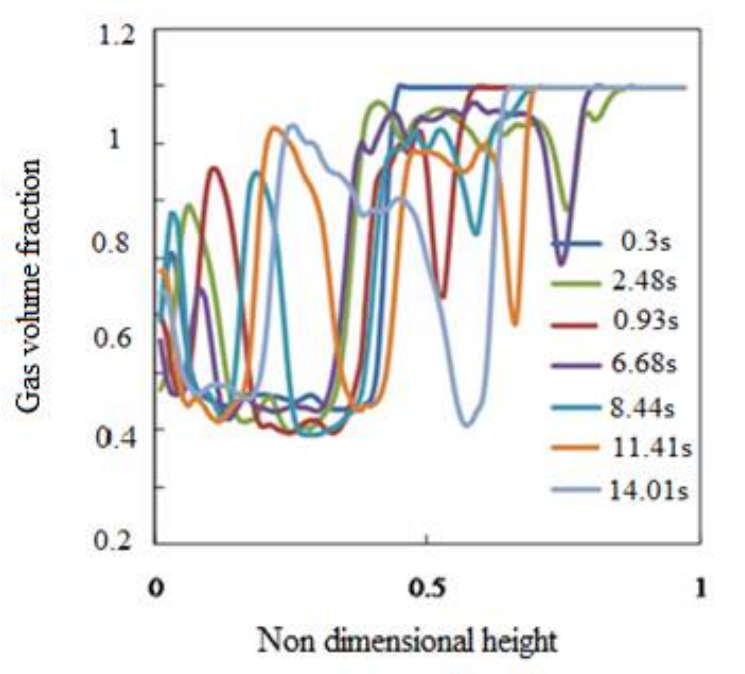

Figure. 4: Variation of gas volume fraction (ε_g) profile with non dimensional height at different times for u_g = 0.28 m/s

Figure. 1 and 3 shows the gas volume fraction for u_g = 0.26 m/s and 0.28 m/s at different times. In Figure 3, variation of void fraction with non dimensional height at different times were presented for u_g = 0.26 m/s. Figure 5(a-b) and Figure 6(a-b) shows the snapshots of the particle motion at various times for u_g= 0.26 m/s and 0.28 m/s. When, the gas injected into the bed the particles moves due to the drag force. As a result, the bed is expanded and fluidized bed height is increased. It was observed that as the superficial velocities increases the bed height also increases. It was observed in the simulation that a small scale bubble appears at the lower part of bed (Figure 1a). The appearance of the bubble kind structure in the fluidized bed within few seconds of injection of gas shows the occurrence of instability in the fluidized bed system. This instability give rises to the formation bubbles of different sizes (Sundaresan., 2003). It was observed that, by increasing the superficial gas velocity, instability appears earlier in the fluidized bed. It was interesting to note that, in case of u_g = 0.26 m/s bubble appears around t = 0.48 s in the lower part of the bed. But, in case of u_g = 0.28 m/s the bubble appears around t = 0.3 s in the lower part of the bed. While moving it was stretched and breaks into smaller bubbles (Figure 1 (a-d)).

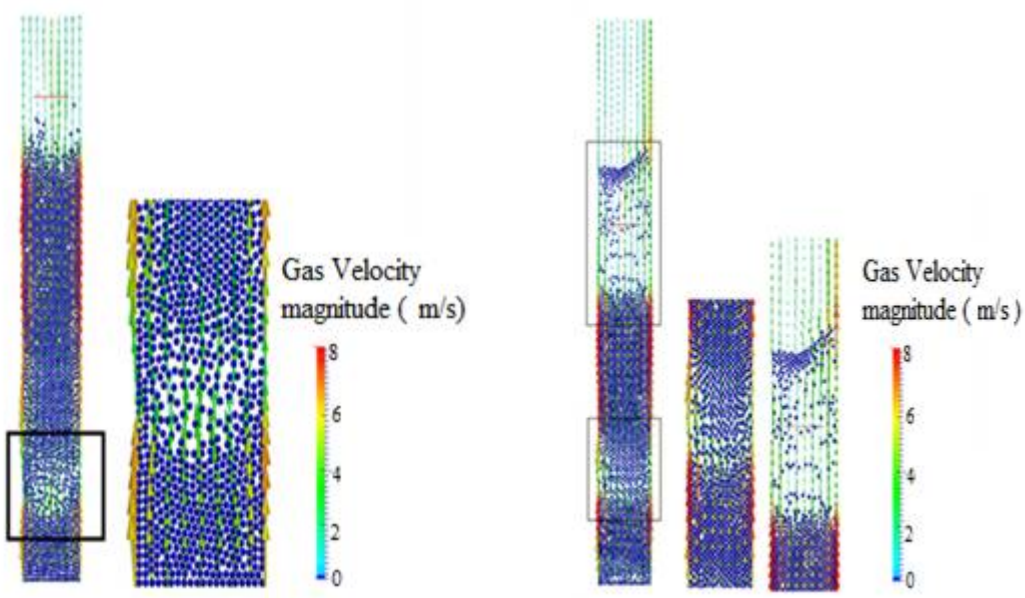

(a) (b)

Figure. 5: Velocity vector plot for u_g = 0.26 m/s (a) 0.48 s (b) 14.17 s

As the bubble moves through the bed, it coalescence to bubble of bigger sizes (Figure 1(d) and (e)). This bubble moves toward the upper part of the bed. During the bed expansion, bubbles of different sizes appear near the wall of the fluidized bed. The presence of bubble of different sizes (both small and large scale) makes the system into multiple bubbling regimes. The presence of bubbles inside the bed pushes the band of particles towards the upper part of the bed. It was clearly observed seen in Figure 5(a-b). It was observed from simulation that, the generations of bubbles are periodic in nature (Figure 1(a-g) and Figure 3(a-g)). It was interesting to note that with the increase in superficial velocity form 0.26 m/s to

0.28 m/s, the size of bubbles of increase (Figure 3 (a-g)). It causes the formation of distinct band of particles inside the bed.

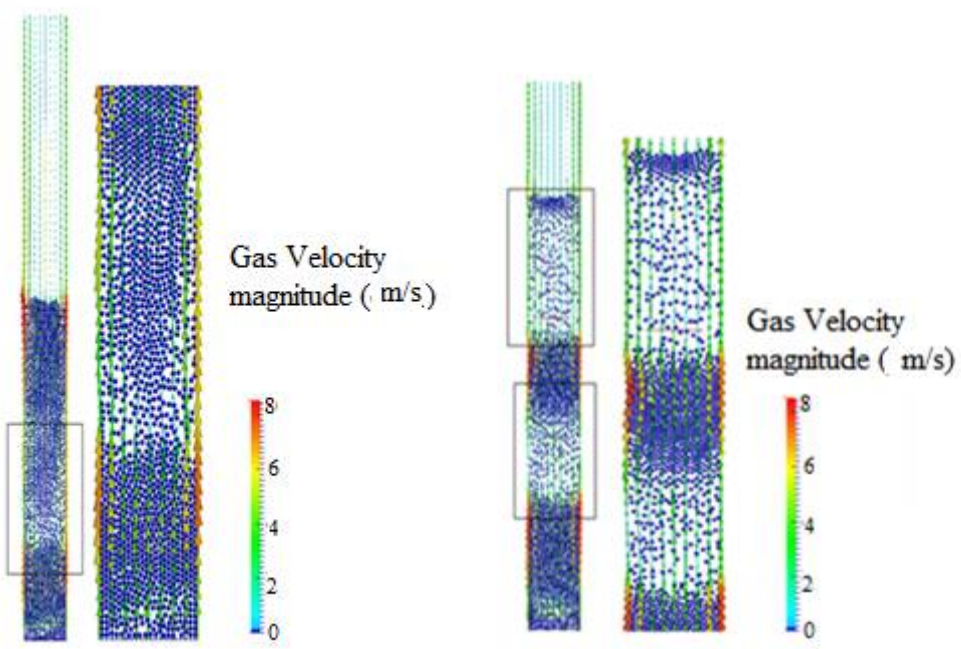

(a) (b)

Figure. 6: Velocity vector plot for u_g = 0.28 m/s (a) 0.3 s (b) 11. 17s

3.2 Power spectra analysis

In the present section, we have presented the power spectrum of the void fraction signal at various heights in a fluidized bed. Figure 7 (a-c) shows the void fraction time series plot for u_g = 0.26 m/s at three different heights (y = 0.055, 0.135 and 0.315 m) in the fluidized bed. The fluctuations of void fractions at various heights show the presence of multi bubbling regimes in the fluidized bed. It is interesting to note that, the amplitude of the signal at the bottom part of the fluidized bed is smaller than to centre part of the fluidized bed. It means with the increase in height, the amplitude of the signal increases. The lower amplitude may due to the appearance of the smaller bubbles in the lower part of the bed (y = 0.055 m). Figure 8 (a-c) shows the void fraction time series plot for u_g = 0.26 m/s at three different heights (y = 0.055, 0.135 and 0.315 m) in the fluidized bed Similarly, the large amplitude near the middle part of the fluidized bed due to the presence of large scale bubbles. It was also observed that when the velocity rises from u_g = 0.26 to 0.28 m/s, the amplitude of the void fraction signal increases. The observed void fraction signal observed in this velocity range is complex and irregular, since the bubble appears coalescence and disappears.

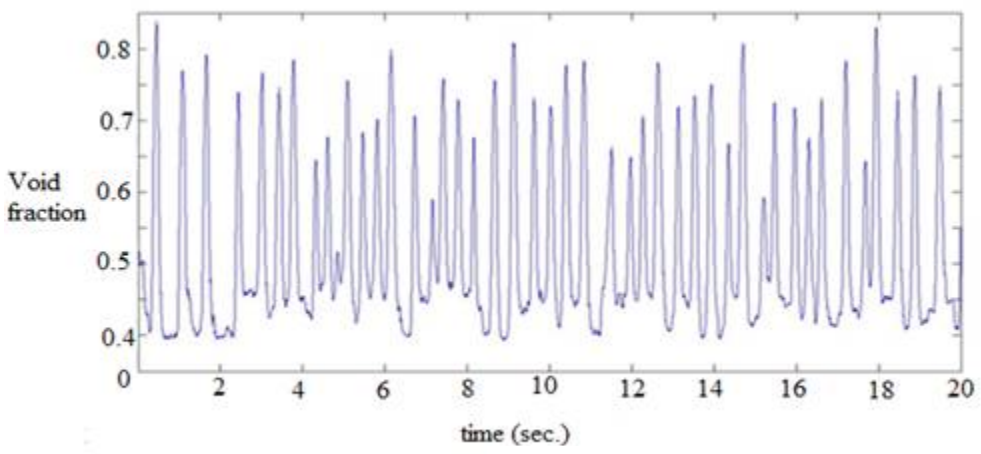

(a)

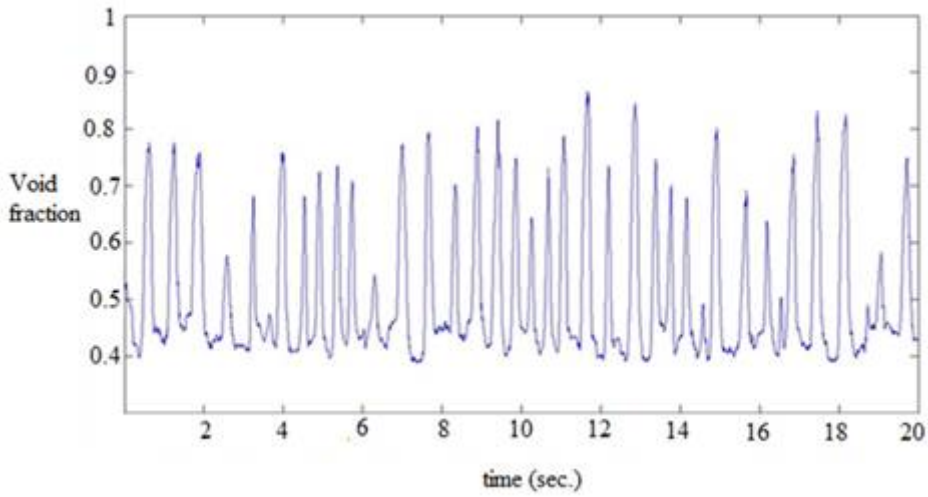

(b)

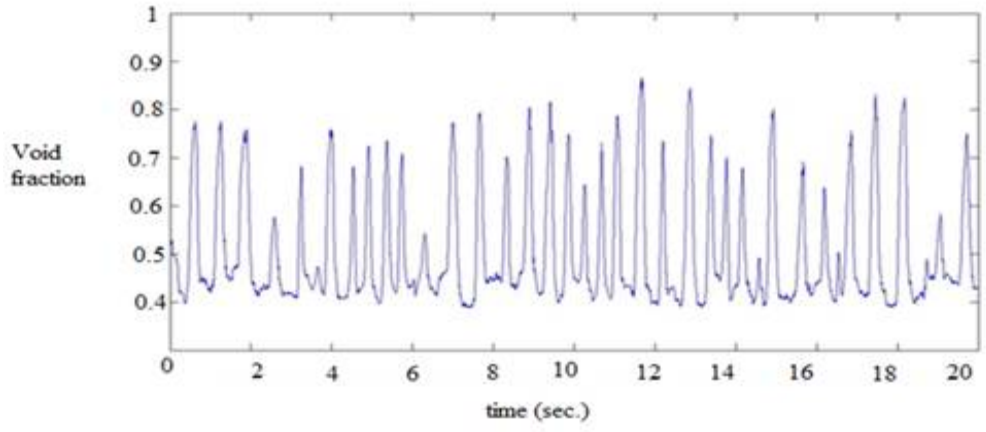

(c)

Figure. 7: Gas void fraction fluctuations signal for u_g = 0.26 m/s at different heights (a) 0.055 m (b) 0.135 m (c) 0.315 m

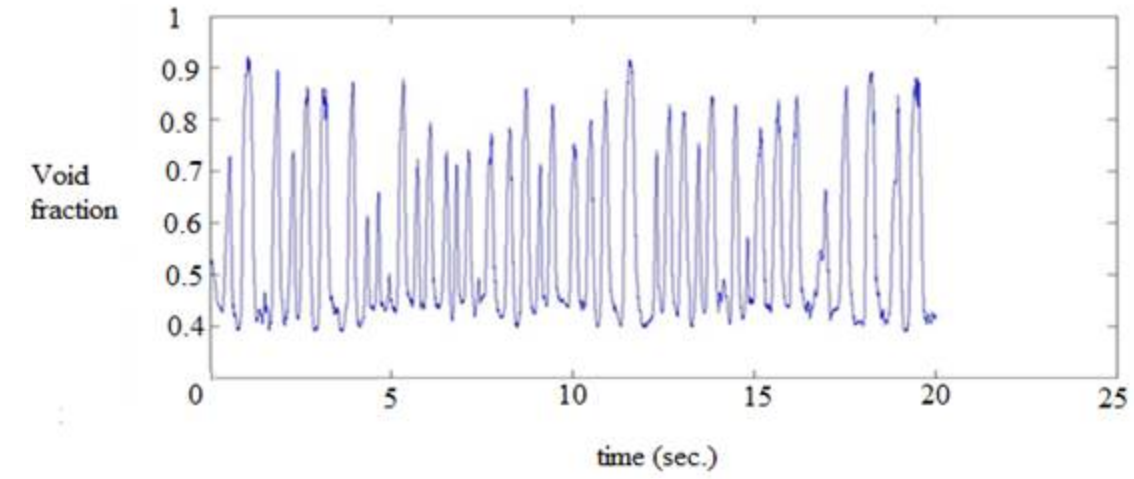

(a)

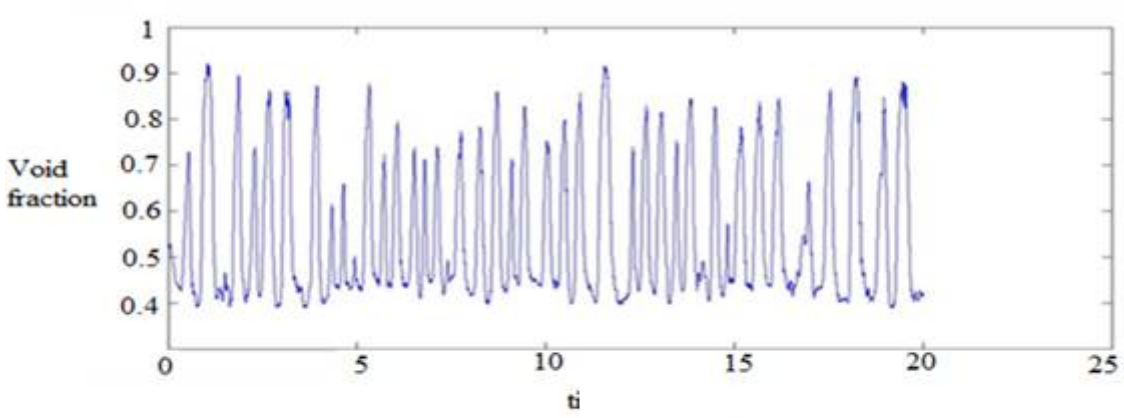

(b)

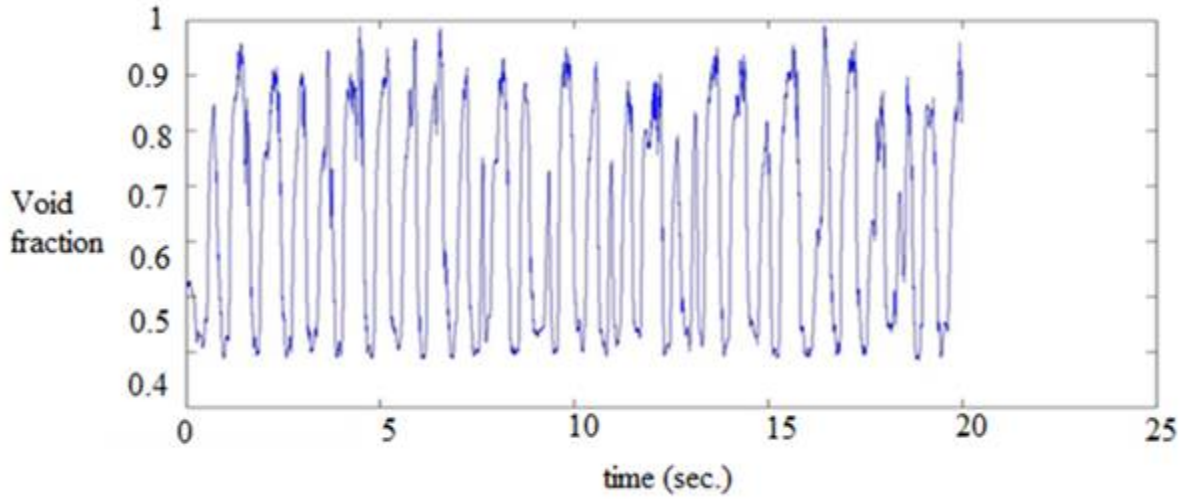

(c)

Figure. 8: Gas void fraction fluctuations signal for u_g = 0.28 m/s at different heights (a) 0.055 m (b) 0.135 m (c) 0.315 m

The power spectrum of the signal first computed by calculating Fourier transforms of the void fraction ε_g *(t)* from the following formula

$$\hat{\varepsilon}_g(f) = \int_0^T \varepsilon_g(t) e^{-i2\pi ft} dt \tag{15}$$

The power spectrum of the signal is computed from the following equation

$$P(f) = \left|\hat{\varepsilon}_g(f)\right|^2 = \left|\int_0^T \varepsilon_g(t) e^{-i2\pi ft} dt\right|^2 \tag{16}$$

Assuming that, $\varepsilon_g(t)$ is sampled at N data points that are equally spaced at a distance Δt. The time of sampling $t_n = n\Delta t$. However it is convenient to begin with n = 0. Thus we have,

$$\hat{\varepsilon}_g(f) = \Delta t \sum_{n=0}^{N-1} \varepsilon_g^{(n)} e^{-i2\pi f_n \Delta t} \tag{17}$$

The discrete version for equation (15) is

$$\varepsilon_g^{(n)} = \varepsilon_g(n\Delta t) \qquad n = 0,1,2,....,(N\text{-}1) \tag{18}$$

The discrete version for equation (15) is

$$\hat{\varepsilon}_g(f) = \Delta t \sum_{n=0}^{N-1} \varepsilon_g^{(n)} e^{-i2\pi f_n \Delta t} \tag{19}$$

The calculation for discrete frequency is calculated from the following equation

$$f_k = \frac{k}{T} = \frac{k}{n\Delta t} \qquad n = 0,1,2,....,(N\text{-}1) \tag{20}$$

At these frequencies, Fourier components are given by

$$\varepsilon_g^{(k)} = \frac{\varepsilon_g(f_k)}{\Delta t} = \sum_{n=0}^{N-1} \varepsilon_g^{(n)} e^{-i\frac{2\pi kn}{N}} \qquad k = 0,1,2,....,(N\text{-}1) \tag{21}$$

An in-house MATLAB code was developed to calculate FFT (Fast Fourier Transform) of the signal.

Figures 9(a-c) and 10(a-c) illustrate six examples of power spectra resulting from gas void fraction fluctuations in the multi bubbling regime. Much wider spectra can be observed in the multiple bubble regimes. Larger peaks in the spectra were observed in the central part of the fluidized bed (Figure 9c and 10c). It was clearly observed that as the velocity of superficial gas velocity increases, the amplitude of these signal increases. There was a continuous passage of bubbles through the bed, and several bubbles erupted simultaneously on the bed surface. These visual observations suggest the occurrence of much wider spectra for the multiple bubble regimes. Another important characteristic of the power spectra profile, observed for both the velocities, was a frequency peak near the centre part of bed (Figure 9c and 10c). This shows that, even in the multiple bubble regimes, one frequency component always stands out from the others.

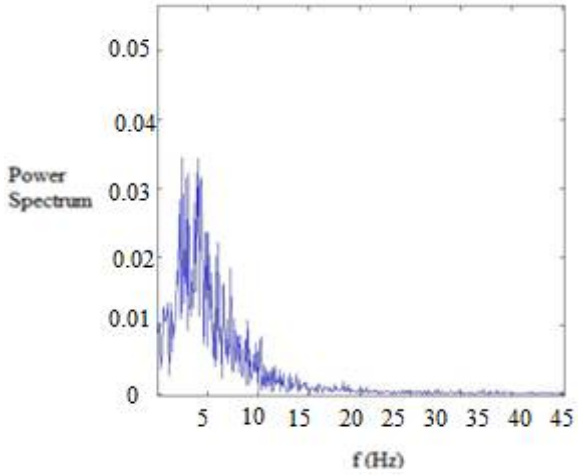

(a)

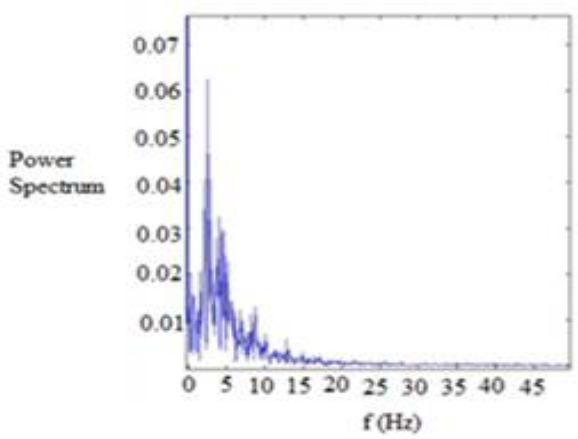

(b)

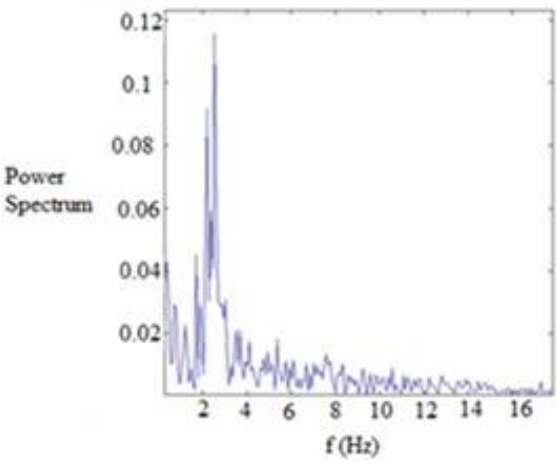

(c)

Figure. 9: Power spectrum for u_g = 0.26 m/s (a) y = 0.055 m (b) 0.135 m (c) 0.315 m

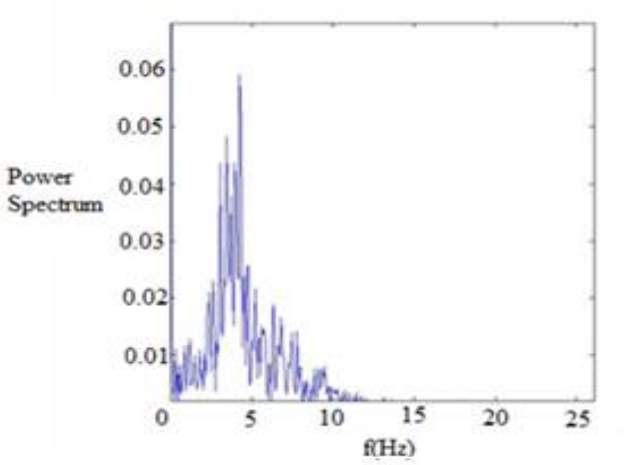

(a)

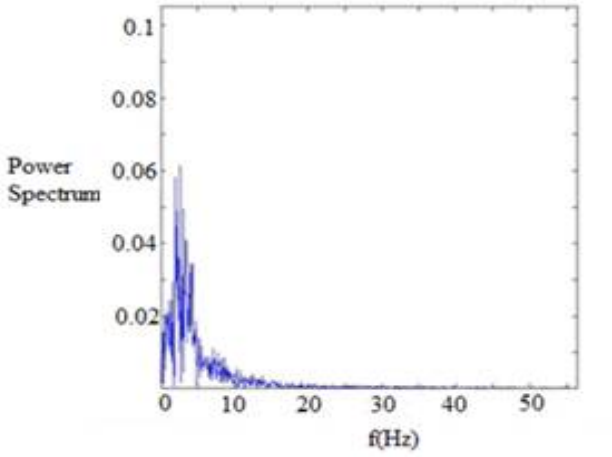

(b)

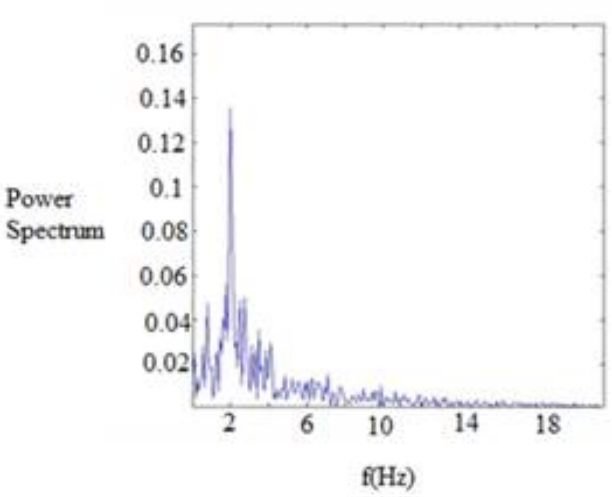

(c)

Figure. 10: Power spectrum for u_g = 0.28 m/s (a) y = 0.055 m (b) 0.135 m (c) 0.315 m

4. CONCLUDING REMARKS

Two dimensional DEM-CFD simulations were performed for the different velocities in a fluidized bed. The following conclusions were made from the above study

- It was observed that the bed height increases with increase in superficial gas velocities.
- The appearance of the bubble kind structure in the fluidized bed within few seconds of injection of gas shows the occurrence of instability in the fluidized bed system. This instability give rise to the formation bubbles of different sizes.
- Multi-bubbling regime was observed in the simulation. Amplitude of the signal increases with increase with gas velocity and height of the bed.
- Much wider spectra can be observed in the multiple bubble regimes. Larger peaks in the spectra were observed in the central part of the fluidized bed. A frequency peak was observed at the centre of the fluidized bed.

In our future work, we have planned to carry out more numerical simulations to investigate the two dimensional instabilites in the fluized bed.

REFERENCES

Alberto, C., Felipe, Rocha.,S.C.S, 2004. Time series analysis of pressure fluctuation in gas solid fluidized beds. *Brazilian journal of Chemical Engineering*, vol.21, n. 3,pp. 497-507.

Anderson, T.B., Jackson, R.,1967. A fluid mechanical description of fluidized beds: Equations of motion, *I&EC Fundamentals*, vol. 6, n. 4, pp. 527-539.

Anderson, K.,Sundaresan, S.,Jackson, R., 1995. Instabilities and the formation of bubbles in fluidized beds, *Journal of Fluid Mechanics*, vol 303, pp. 327–366.

Batchelor, G.K., 1988. A new theory of the instability of a uniform fluidized bed, *Journal of Fluid Mechanics* 193, pp. 75–110.

Bendat, J.S., & Piersol, A.G, 1986. Analysis and Measurement Procedures, John Wiley & Sons, New York.

Cundall, P.A., Strack, O.D.L. 1979. A discrete numerical model for granular assemblies, *Geotechnique*, vol. 29 , 47–65.

Cunha, F. R., Sobral, Y. D., Gontijo, R. G. 2013. Stabilization of concentration waves in fluidized beds of magnetic particles. *Powder Technology*, vol. 24, pp. 219-229.

Das, Shyam.S., Sobral, Y.D., Cunha, F.R.2016. CFD-DEM simulations of Gas-Solid Fluidized beds. CNMAC 2016, Gramado, Brazil.

Duru, P.,Guazzelli, E., 2002. Experimental investigation on the secondary instability of liquid-fluidized beds and the formation of bubbles, *Journal of Fluid Mechanics*, vol. 470 , pp.359–382.

EL-Kaissy, M.M, Homsy, G.M., 1976. Instability waves and the origin of bubbles in fluidized beds. *International Journal of Multiphysics flows*, vol. 2, pp:379-395.

Fortes, A.F., Joseph, D.D.,Lundgren, T.S, 1987. Nonlinear mechanics of fluidization of beds of spherical particles, *Journal of Fluid Mechanics*, vol. 177, pp.467–483.

Garg, R., Galvin, J., Li, T., Pannala, S., 2012. Open-source MFIX-DEM software for gas-solids flows: Part I – verification studies, *Powder Technology* , vol. 220, pp:122–137.

Garg, R.,Galvin, J, Li, T., Pannala, S., 2012.Open-source MFIX-DEM software for gas-solids flows: Part II – verification studies, *Powder Technology*, vol. 220, pp.138–150.

Glasser, B.J., kevrekidis, I.G., Sundarresen, S., 1996. One and two dimesional travelling wave solutions in a gas fluidized beds. *Journal of fluid Mechanics*, vol. 306, pp: 183-221.

Lim, E.W.C. , Wong, Y.S., Wang, C.H., 2007. Particle image velocimetry experiment and discrete-element simulation of voidage wave instability in a vibrated liquid-fluidized bed. *Industrial and Engineering Chemistry Research*, vol. 46, pp.1375–1389.

Patankar, S., 1980. Numerical Heat Transfer and Fluid Flow. Hemisphere Publishing Corporation.

Sergeev, Y.A. 1995. Linear and Non-linear Concentration Waves in Magnetically Stabilized Fluidized Beds, *Mobile Particulate Systems*, NATO ASI Series,vol. 287,pp. 249–260.

Sobral, Y.D, Hinch, E.J., 2011. Gravitational overturning in stratified particulate flows,*SIAM Journal on Applied Mathematics*, vol. 71, pp.2151–2167.

Sobral, Y.D., Cunha F.R., 2003. A stability analysis of a magnetic fluidized bed, *Journal of Magnetism and Magnetic Materials*, vol. 258/259, pp. 464–467.

Sobral, Y.D.,Oliveira, T.F,Cunha, F.R.,2007. On the unsteady forces during the motion of a sedimenting particle, *Powder Technology*, vol 178, , pp.131–143.

Sobral, Y. D., 2008. *Instabilities in fluidised beds*, Ph.D Thesis, Department of Applied Mathematics and Theoretical Physics , University of Cambridge, England.

Sobral, Y.D., Cunha,F.R., 2002. A linear stability analysis of a homogeneous fluidized bed, *Tendencies in Computational and Applied Mathematics*, vol. 3, pp. 197–206.

Sundaresan. S.,2003. Instabilities in fluidized beds, *Annual Review of Fluid Mechanics*, vol. 35, pp 63–88.

Syamlal, M. 1998. Mfix documentation: Numerical guide. Tech. Rep. DOE/MC31346-5824, NTIS/DE98002029,National Energy Technology Laboratory, Department of Energy.

Tsuji , Y.,Kawaguchi , T.,Tanaka, T.,1993. Discrete particle simulation of two dimensional fluidized bed, *Powder Technology*, vol. 77, pp. 79-87.

Wang, S., Sun, Z.,Li, X.,Gao, J., Lan, X., Dong, Q., 2013. Simulation of flow behavior of particles in liquid–solid fluidized bed with uniform magnetic field, *Powder Technology*, vol. 237,pp. 314–325.

Van Leer, B., 1979.Towards the Ultimate Conservative Difference Scheme, V. A Second Order Sequel to Godunov's Method, *J. Com. Physics.*, vol. *32*, pp. 101–136.